Journal of Inorganic Biochemistry 276 (2026) 113164

Contents lists available at ScienceDirect

Journal of Inorganic Biochemistry

journal homepage: www.elsevier.com/locate/jinorgbio

The *Neisseria gonorrhoeae* cytochrome c_2-bacterial peroxidase electron-transfer complex is competent in hydrogen peroxide reduction

Pedro M.S. Bragança [a,b], Daniela S. Barreiro [a,b], Marta S.P. Carepo [c,d], Sofia R. Pauleta [a,b,*]

[a] Microbial Stress Lab, UCIBIO, Chemistry Department, Faculdade de Ciências e Tecnologia, Universidade NOVA de Lisboa, Campus da Caparica, 2829-516 Caparica, Portugal
[b] Associate Laboratory i4HB – Institute for Health and Bioeconomy, Faculdade de Ciências e Tecnologia, Universidade NOVA de Lisboa, Portugal
[c] LAQV-REQUIMTE, Chemistry Department, Faculdade de Ciências e Tecnologia, Universidade NOVA de Lisboa, Campus da Caparica, 2829-516 Caparica, Portugal
[d] Escola de Psicologia e Ciências da Vida, Departamento de Ciências da Vida, Universidade Lusófona, Campo Grande 376, 1749-024 Lisboa, Portugal

ARTICLE INFO

Keywords:
Neisseria gonorrhoeae
Reactive oxygen species
c-type cytochrome
Bacterial peroxidase
Steady-state kinetics
Electron-transfer complex

ABSTRACT

Neisseria gonorrhoeae is a pathogenic bacterium responsible for the disease gonorrhea, which has gained increasing attention in recent years due to the emergence of strains resistant to the currently used antibiotics. In the absence of a vaccine, understanding mechanisms that contribute to infection is imperative. One such mechanism is the reduction of hydrogen peroxide by the outer membrane bound bacterial peroxidase. Here, steady-state kinetics shows that cytochrome c_2, previously implicated in nitrite reduction, is an efficient electron donor to this enzyme, proving to be an alternative to the lipid-modified azurin. The cytochrome c_2-mediated peroxidase activity has a K_M of 0.74 ± 0.08 μM and a k_{obs} of 18 ± 1 s^{-1} for hydrogen peroxide, with an optimum pH at 7.7. The pH and ionic-strength dependence of this activity differs from that of azurin, suggesting that the two electron donors can play complementary roles depending on external conditions. Furthermore, the viscosity dependence of the activity suggests that protein-protein interactions are not purely diffusion-controlled but also governed by conformational changes required for complex formation and/or electron transfer, and docking analysis implies that cytochrome c_2 binds near the exposed edge of the electron transferring heme of the bacterial peroxidase.

This study improves our understanding of the periplasmic physiology of *N. gonorrhoeae* by demonstrating how the pathogen's flexibility in using electron donors enables it to maintain peroxidase activity and cope with oxidative stress in different host environments. These insights could inform future strategies aimed at disrupting redox homeostasis to combat antibiotic-resistant strains.

1. Introduction

The obligatory human pathogen *Neisseria gonorrhoeae* is responsible for the sexually transmitted infection gonorrhea and according to the World Health Organization, approximately 87 million new cases of gonorrhea infection were reported globally in 2016 [1].

The antimicrobial resistance exhibited by *N. gonorrhoeae* represents a major public health threat and underscores the urgent need for the development of new antimicrobial agents [2]. In response to these challenges, new therapeutic targets, such as the bacteria's defense mechanisms towards the host immune responses and neighboring microorganisms, are increasingly being explored [3–5].

During infection, this pathogen is often subjected to oxidative stress caused by reactive oxygen species (ROS) produced by the host's defense mechanisms, such as hydroxyl radical (HO•), hydrogen peroxide (H_2O_2) and superoxide anion (O_2^-) [6]. *N. gonorrhoeae* oxidative stress response involves several transcriptional regulators and defense proteins tailored to detoxify both endogenous and exogenous ROS [7–10]. Exogenous ROS, mainly H_2O_2, is generated during the macrophagic oxidative burst and tissue inflammation associated with gonococcal infection and proliferation [9]. in In *N. gonorrhoeae* the main H_2O_2 scavengers are catalase (KatA) [11] and the bacterial peroxidase (BCCP) [12,13].

N. gonorrhoeae bacterial peroxidase is an outer membrane-bound classic bacterial peroxidase encoded by the *ccp* gene, that catalyzes the reduction of hydrogen peroxide to water, using the lipid-modified azurin as electron donor [14,15]. The expression of the *ccp* gene is

* Corresponding author at: Microbial Stress Lab, UCIBIO, Chemistry Department, Faculdade de Ciências e Tecnologia, Universidade NOVA de Lisboa, Campus da Caparica, 2829-516 Caparica, Portugal.
E-mail address: sofia.pauleta@fct.unl.pt (S.R. Pauleta).

https://doi.org/10.1016/j.jinorgbio.2025.113164
Received 11 September 2025; Received in revised form 18 November 2025; Accepted 24 November 2025
Available online 25 November 2025

induced in low oxygen environments as it is under the regulation of the anaerobic transcription factor Fumarate and Nitrate reduction Regulator (FNR) [10]. Since the globular domain of the bacterial peroxidase is located in the periplasm, it is regarded as the first line of defense against exogenous H_2O_2 [6]. This assertion is supported by the fact that a *ccp/katA* double-mutant is more sensitive to H_2O_2 under anaerobic conditions in comparison to a *katA* single-mutant [16].

The bacterial peroxidase has two *c*-type hemes in two distinct domains, each of which has a cytochrome fold (Fig. 1A). The heme in the C-terminal domain was named electron transferring heme (E heme), and the heme in the N-terminal domain was named peroxidatic heme (P heme) (Fig. 1A) [17]. The E heme has a reduction potential of around +300 mV at pH 7.5 and has a His/Met coordination in a low/high-spin equilibrium at room temperature (Fig. 1B) [12,17]. Its function is to receive electrons from small redox proteins and to transfer them to the P heme. The P heme has a reduction potential of −300/−190 mV at pH 7.5 [12], and is low-spin and bis-histidine coordinated when the enzyme is isolated in the oxidized state. It is the catalytic center where the reduction of hydrogen peroxide occurs [12,17]. However, reductive activation is required for this to be possible, whereby the distal histidine is lost from the P heme (Fig. 1B). This is a calcium-dependent process initiated by the reduction of the E heme, triggering conformational changes in the polypeptide chain [12,17]. These changes displace the distal axial histidine ligand of the P heme, resulting in the formation of a penta-coordinated high-spin heme that is accessible to the substrate [12,17].

As mentioned, classic bacterial peroxidases use small redox proteins as electron donors. These electron shuttle proteins are either *c*-type cytochromes or type 1 copper proteins, from the azurin or pseudoazurin subfamilies [18–26].

N. gonorrhoeae has both types of redox proteins in the periplasm, a *c*-type cytochrome, cytochrome c_2 [27] (Fig. 1C), and a lipid-modified azurin (LAz) [28]. LAz is a small cupredoxin lipid-anchored to the outer membrane *via* an N-terminal palmitoyl modified cysteine residue and exhibits the typical cupredoxin fold [15], while cytochrome c_2 is a small, soluble, monohemic cytochrome encoded by the *cccA* gene [27], proposed to be involved in respiration under low oxygen tensions [27]. Previous kinetic studies determined turnover numbers (k_{obs}/[Laz]) of 3.9 $\mu M^{-1}.s^{-1}$, and K_M of 0.4 μM for hydrogen peroxide, with optimum catalytic activity observed at 37 °C and pH 6.0–7.5 [14], which closely matches the physiological conditions of *N. gonorrhoeae*. This electron-transfer complex is driven by hydrophobic interactions, which facilitates dissociation and allows a high turnover. Its model structure predicted LAz binding near the E heme of the bacterial peroxidase [14].

The coexistence of *c*-type cytochromes and cupredoxins in the periplasm of certain Gram-negative bacteria under low oxygen tensions has led to the hypothesis that these two types of electron shuttle can both donate electrons to enzymes from the denitrification pathway and to bacterial peroxidases [25,29,30]. In the case of *Pseudomonas aeruginosa*, *Paracoccus pantotrophus* and *Paracoccus denitrificans* both *in vitro* and *in vivo* evidence supports this proposal [20,25,29,30]. While *N. gonorrhoeae* cytochrome c_2 has been shown to be involved in the electron-transfer pathway required for nitrite reduction [27], evidence of its involvement in either *in vivo* or *in vitro* hydrogen peroxide reduction is lacking, a gap that will be addressed here for the latter.

In this study, the kinetic parameters of cytochrome c_2-mediated hydrogen reduction by *N. gonorrhoeae* bacterial peroxidase were determined, showing that this protein is a competent electron donor to this enzyme. The electron-transfer complex was structurally characterized using molecular docking. These results improve our understanding of *N. gonorrhoeae* physiology and electron-transfer pathway under infection-like conditions.

2. Materials and methods

2.1. Heterologous production and purification of bacterial peroxidase and cytochrome c_2

Bacterial peroxidase was heterologously produced and purified as described in [12]. The final protein sample had a purity ratio A_{403nm}/A_{280nm} above 4.0 and an expression yield of 8.2 mg pure protein per L of growth media. The samples were stored in 25–50 μL aliquots at −80 °C. The concentration of the bacterial peroxidase was determined using the extinction coefficient at 402 nm of 222 mM^{-1} cm^{-1}, in the oxidized state [12].

Cytochrome c_2 encoding gene (*cccA*) was codon optimized for heterologous production in *Escherichia coli*. The first 21 codons encoding the native signal peptide were removed. The *cccA* gene was cloned into the pET22b(+) expression vector, and hereby named pET22b_*Ng*Cytc$_2$. The sequence was cloned within the restriction sites *Nco*I, downstream of the *pelB* sequence, and *Xho*I. The expression vector confers ampicillin resistance and adds a signal peptide (*pelB*) of 21 residues to the N-terminus of the encoding gene, to signal the protein to the periplasm. The cloning strategy introduced only a Met in the N-terminus in the mature protein. Cytochrome c_2 was produced in *E. coli* BL21(DE3) (NZYtech) competent cells co-transformed with pET22b_*NgcccA* and pEC86 (harboring the *ccm* genes that encode the machinery responsible for the biosynthesis/maturation of a functional *c*-type cytochrome and confers chloramphenicol resistance). Cytochrome c_2 was produced in *E. coli* BL21(DE3) as described for the bacterial peroxidase [12], only changing the concentration of isopropyl β-D-thiogalactopyranoside (IPTG) used to induce gene expression to 0.8 mM, and the buffer used to resuspend the cells (50 mM Tris-HCl, pH 8.0, due to the high pI 9.2 of cytochrome c_2). The periplasmatic fraction was obtained by 5 freeze-thaw cycles and separated from the spheroplasts and cell debris at 48000 g, 45 min, 6 °C. The periplasmic extract was diluted 5 × with cold Milli-Q water and

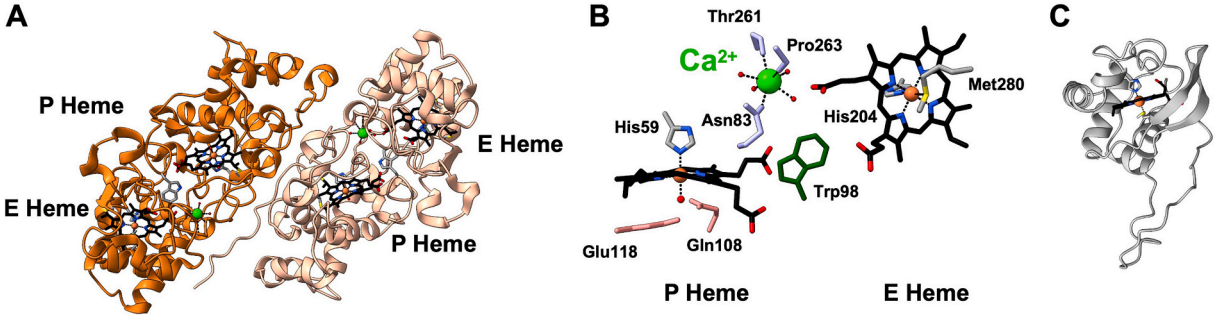

Fig. 1. Structural representation of the proteins studied here, bacterial peroxidase (panel A and B) and cytochrome c_2 (panel C) from *Neisseria gonorrhoeae*. Panel **(A)** shows the bacterial peroxidase in the mixed-valence state with the backbone of each monomer colored differently, and the hemes represented as sticks colored by element. Panel **(B)** shows the coordination of the hemes, calcium ion and residues proposed to be involved in electron transfer between the two heme (Trp98) and catalysis (Glu118 and Gln108), represented as sticks colored by element. Panel **(C)** shows the AlphaFold model of cytochrome c_2, with the backbone colored in white, with the heme and heme iron coordinating residues as sticks colored by element. Panel A and B were prepared using the coordinates PDB ID 7ZS8.

loaded onto a 5 mL HiScreen SP Sepharose Fast Flow column (Cytiva) equilibrated with 50 mM Tris-HCl pH 8.0. The unbound proteins were eluted with 10 mM Tris-HCl, pH 8.0, and cytochrome c_2 was eluted with a linear gradient between 0 and 500 mM NaCl in 10 mM Tris-HCl, pH 8.0. The fractions with A_{410nm}/A_{280nm} above 7.0 were combined and concentrated over a 3 kDa MWCO Amicon® ultra centrifugal filter and the buffer was exchanged to 20 mM Tris-HCl, pH 7.6, using a desalting PD-10 column (Cytiva). A 12.5 % Tris-Tricine SDS-PAGE stained for protein (Coomassie blue) and heme content [31] was also used to evaluate protein purity. The final cytochrome c_2 sample had a purity ratio above 7.0 and was stored in 500 μL aliquots at −80 °C, until further use. This production protocol had a yield of 20 mg of purified protein per L of growth media. For the kinetic assays cytochrome c_2 was reduced with 2 mM sodium ascorbate and 5 μM 3,6-diaminodurol (DAD) for 30 min at room temperature under an inert atmosphere. The reducing agent and DAD were removed inside a MBraun glove box using a desalting column, NAP-5 (Cytiva), equilibrated with 10 mM of 2-(N-morpholino) ethanesulfonate (MES) buffer, pH 6.5, 10 mM NaCl and 1 mM $CaCl_2$. The final protein concentration was determined using the extinction coefficient of the reduced cytochrome c_2 at 553 nm (ε_{553nm} of 22.9 $mM^{-1}.cm^{-1}$).

The SDS-PAGE and visible spectra of the purified bacterial peroxidase and cytochrome c_2 are presented in Supplementary Materials S1.

2.2. Kinetic assays with cytochrome c_2 as electron donor

The activity of the bacterial peroxidase using reduced cytochrome c_2 as an electron donor was determined by monitoring the decrease in the absorbance at 553 nm over time, in a TIDAS diode array inside a MBraun glove box. In all kinetic assays, *N. gonorrhoeae* bacterial peroxidase was pre-activated. For that 5 μM enzyme solution in 10 mM 4-(2-hydroxyethyl)-1-piperazineethanesulfonate (HEPES), pH 7.5, 10 mM NaCl, 1 mM $CaCl_2$, 0.2 mM sodium ascorbate and 5 μM DAD, was incubated during 30 min at room temperature under inert atmosphere [12].

The assays were performed inside the glove box, at 25 °C, in 10 mM MES, pH 6.5, 10 mM NaCl and 1 mM $CaCl_2$, containing 10 μM reduced cytochrome c_2, 100 μM H_2O_2, and initiated with 10 nM pre-activated bacterial peroxidase. At the end of each assay, a small aliquot of potassium ferricyanide was added to fully oxidize cytochrome c_2 to confirm that the electron donor was completely oxidized at the end of the assay. To establish the concentration of enzyme to be used in the kinetic studies, assays were performed at pH 6.5, with 100 μM H_2O_2 in the presence of 5 to 50 nM pre-activated bacterial peroxidase. To determine the kinetic parameters relative to H_2O_2, H_2O_2 concentration ranged between 2.5 and 500 μM in the same assay conditions. The dependence on the concentration of reduced cytochrome c_2 was also studied between 1.5 and 16 μM, in an assay mixture composed by 10 mM MES, pH 6.5, 10 mM NaCl, 1 mM $CaCl_2$, 100 μM H_2O_2 and initiated with 10 nM pre-activated enzyme. The pH dependence of the peroxidase activity was assessed by varying the buffer pH at a concentration of 10 mM with 10 mM NaCl and 1 mM $CaCl_2$ (MES buffer with pH 5.5 to 6.5; HEPES buffer with pH 6.5 to 8.0; 3-([1,1-dimethyl-2-hydroxyethyl] amino)-2-hydroxypropanesulfonate (AMPSO) buffer with pH 8.0 to 9.5). The pH dependence was not assessed at pH values below 5.5 and above 9.5 because of the stability of both proteins. The ionic strength dependence was evaluated by adding NaCl to the assay buffer between 0 and 500 mM, and the effect of viscosity was assessed by adding glycerol to the assay buffer between 0 and 30 % glycerol. The viscosity values of these solutions were taken from [32]. These assays were performed in the presence of 100 μM H_2O_2 and initiated with 10 nM pre-activated enzyme.

All the assays were performed at least in triplicates, and the values reported are the average with the associated error. The observed initial velocities, V_0, were determined by the difference between the slope, in the first seconds of the cytochrome c_2 oxidation, after enzyme addition and the slope of the oxidation of cytochrome c_2 in the presence of hydrogen peroxide. The pH dependence data was fitted using a bell-shaped function [33] with Eq.1.

$$V_0 = \frac{V_{max}\left(\beta_1 + \beta_2 \cdot \frac{Ka_1}{[H^+]} + \beta_3 \cdot \frac{Ka_1 Ka_2}{[H^+]^2}\right)}{1 + \frac{Ka_1}{[H^+]} + \frac{Ka_1 Ka_2}{[H^+]^2}} \quad (1)$$

in which the reaction rate, V_0, is given as a function of $[H^+]$ considering two K_a values and three β values. In this case, β_1 and β_3 were 0, and β_2 has 1.

2.3. Bioinformatic analysis of the structures

The protein electrostatic surface was analyzed using Adaptive Poisson-Boltzmann Solver (APBS [34,35]). The PDB files were treated in PDB2PQR [36] (http://nbcr-222.ucsd.edu/pdb2pqr_2.1.1/). The final PQR file from PDB2PQR was used as input in the APBS (http://www.poissonboltzmann.org/) to determine electrostatic properties using default parameters. The solvent accessible surface was colored according to electrostatic potential in ChimeraX 1.9, from −5 to +5 kT/e (red to blue). The hydrophobic surface was rendered in Discovery Studio 2021, colored from non-hydrophobic residues, in green, to hydrophobic residues, in magenta (−3 to +3: color scale green-white-magenta).

2.4. Molecular docking simulation

Two docking algorithms were used to obtain a structural model of the bacterial peroxidase-cytochrome c_2 complex: ZDOCK [37] and HADDOCK (High Ambiguity Driven protein-protein Docking) [38]. The bacterial peroxidase dimer in the mixed-valence state (PDB ID 7ZS8) was considered the target and the probe was the structural model of cytochrome c_2 obtained using Alphafold3 server (the confidence of the model is shown in Supplementary Materials S3, Fig. S5) [39]. ZDOCK is a Fast Fourier Transform-based protein docking program, which performs a rigid-body simulation ("hard-dock") in the ZDOCK web-based server 3.0.2 (https://zdock.wenglab.org/). ZDOCK output consisted of 2000 models with a combined score based on shape complementary, electrostatics and desolvation energies, however, only the top five models were analyzed. HADDOCK is an information-driven flexible docking approach ("soft-dock") for the modelling of biomolecular complexes in the HADDOCK web-based 2.4 server (https://rascar.science.uu.nl/haddock2.4/). HADDOCK scores the complexes by a linear combination of buried surface area and several energy scores, such as van der Waals, electrostatic, distance restraints, radius of gyration restraint, direct residual dipolar coupling restraint, intervector projection angle restraints, pseudo contact shift restraint, diffusion anisotropy, dihedral angle restraints, symmetry restraints energy, binding energy and desolvation energy. In this case the top five models were analyzed. AlphaFold3 (https://alphafoldserver.com/) [39] was also used to generate 5 structures of the cytochrome c_2/bacterial peroxidase complex using their mature sequence and indicating the presence of *c*-type hemes as cofactors.

The protein-protein interface analysis of all the complexes was performed in the PDBePISA web server [40], which calculate the geometrical and physicochemical properties according to Jones & Thornton [41]. The electron-transfer pathway was analyzed using the online platform eMAP (https://emap.bu.edu/) [42].

3. Results

3.1. Steady-state kinetics using cytochrome c_2 as electron donor

The cytochrome c_2-mediated catalysis of bacterial peroxidase was studied in continuous assays following the oxidation of the reduced cytochrome c_2 at 553 nm in the presence of enzyme and hydrogen

peroxide (Fig. 2A). The kinetic trace presented in Fig. 2A shows that upon addition of hydrogen peroxide, cytochrome c_2 is oxidized with a low rate (0.022 ± 0.002 μM/s), that increases significantly upon addition of pre-activated bacterial peroxidase. These results demonstrate that cytochrome c_2 can donate electrons to the bacterial peroxidase, while it catalyzes hydrogen peroxide reduction, supporting its role as a physiological electron donor in alternative to LAz.

To establish the enzyme concentration to be used in the kinetic studies, assays were performed varying bacterial peroxidase from 0 to 50 nM, as described in the Materials and Methods. The concentration chosen was 10 nM, at which the steady-state conditions are met as the concentration of both substrates, 100 μM H_2O_2 and 10 μM cytochrome c_2, are >1000 [BCCP]. In fact, this concentration of enzyme falls within the linear region of the graph (Fig. 2B).

The kinetic parameters for the cytochrome c_2-mediated bacterial peroxidase catalytic activity, for the reduction of hydrogen peroxide, were obtained from the fitting of the initial velocities at increasing concentrations of H_2O_2 (Fig. 3A) at pH 6.5 to the Michaelis-Menten equation. This experiment was performed at this pH as it was previously established to be the optimum pH of this enzyme [12,14]. The kinetic parameters determined were a K_M of 0.74 ± 0.08 μM of H_2O_2 and a V_{max} of 0.18 ± 0.01 μM/s, at pH 6.5 and 25 °C. Considering the concentration of enzyme, the k_{obs} was determined to be 18 ± 1 s^{-1}. Compared to previous studies, the K_M decreased one order of magnitude compared to the $ABTS^{2-}$-mediated catalysis (4 ± 1 μM) and was very similar to the K_M of the LAz-mediated catalysis (0.4 ± 0.2 μM). This shows the high affinity of the bacterial peroxidase for H_2O_2 when either of the biological electron donors are used as electron donors. However, the k_{obs} is half the value of the *N. gonorrhoeae* LAz/BCCP pair (39 s^{-1} for LAz), and four-times lower than the k_{obs} of the bacterial peroxidase using $ABTS^{2-}$ as electron donor (79 s^{-1}).

The dependence of the initial velocity on cytochrome c_2 was also studied (Fig. S3 in Supplementary Materials S2), showing a hyperbolic tendency with a K_M > 50 μM, similar to the values estimated for the mediated catalysis of other redox pairs involving bacterial peroxidases: *R. capsulatus* cytochrome c_2/BCCP (K_M ~ 60 μM) [22], *P. pantotrophus* pseudoazurin/BCCP (K_M ~ 70 μM) [21], *Pseudomonas stutzeri* cytochrome c_{551}/BCCP (K_M ~ 54 μM) [24], *P. aeruginosa* cytochrome c_{551}/BCCP (91 μM) [25], and *Methylococcus capsulatus* cytochrome c_{555}/BCCP (61 μM) [26].

Therefore, since cytochrome c_2 was not used in saturating conditions, to compare the kinetic parameters of *N. gonorrhoeae* bacterial peroxidase relative to H_2O_2 with those of other bacterial peroxidases, the k_{obs} was corrected for the electron donor concentration, by k_{obs}/[ED], which gives an effective biomolecular rate constant. This correction is appropriate given that the [ED] used in the assays is well below its anticipated K_M value and under these conditions, the reaction rate is linearly proportional to [ED] (Fig. S3 in Supplementary Materials S2).

The k_{obs}/[Cytochrome c_2] was estimated to be 2 $\mu M^{-1}.s^{-1}$ (pH 6.5), which is of the same order of magnitude as those determined for *N. gonorrhoeae* LAz/BCCP (3.9 $\mu M^{-1}.s^{-1}$, pH 6.0) [14], *Rhodobacter capsulatus* cytochrome c_2/BCCP (2 $\mu M^{-1}.s^{-1}$) [22], and *Methylococcus capsulatus* cytochrome c_{555}/BCCP (5 $\mu M^{-1}.s^{-1}$) [26] but lower than those of *Shewanella oneidensis* cytochrome c_5/BCCP (18 $\mu M^{-1}.s^{-1}$, pH 6.0) [23], *P. aeruginosa* cytochrome c_{551}/BCCP (13 $\mu M^{-1}.s^{-1}$) [25], and *P. stutzeri* cytochrome c_{551}/BCCP (11 $\mu M^{-1}.s^{-1}$, pH 7.5) [24].

The pH dependence of the mediated catalytic activity was studied between 5.5 and 9.5 at saturating concentrations of H_2O_2 (Fig. 3B). The activity profile exhibited a bell-shaped curve, consistent with the presence of two ionizable groups whose protonation state is critical for product formation. The p*Ka* values estimated from the fitting of the data to Eq. 1, were a pKa_1 of 5.8 ± 0.2 and pKa_2 of 9.6 ± 0.1, with an optimum pH of 7.7. The optimum pH is the highest reported in the literature for bacterial peroxidases in which pH-dependence of activity has been determined [43]. The ionizable groups, with p*Ka* of 5.8 and 9.6, may either participate in the formation of a competent electron-transfer complex or be directly involved in the catalytic cycle, as will be discussed.

The ionic strength dependence of the catalytic activity was studied by increasing the concentration of NaCl in the buffer assay (Fig. 3C). The activity profile shows a steady increase in activity up to 100 mM NaCl, reaching 2.3-fold increase of its activity in the absence of NaCl, and remains constant from 100 to 500 mM. This suggests that moderate ionic strength enhances enzyme activity, suggesting that unfavorable electrostatic interactions are shielded, enabling the stabilization of the active conformation of the electron-transfer complex governed by hydrophobic interactions.

The effect of solution viscosity on catalytic activity can provide insight into the rate-limiting step. The solution viscosity was changed by adding glycerol (0–30 %) to the buffer assay at pH 6.5 and 25 °C (Fig. 3D). The presence of 0 to 5 % glycerol (η of 1.0387 mPa·s [32]) has only a marginal effect on the enzyme activity, while at higher values the activity decreases drastically, being inversely proportional to viscosity (Fig. S4 in Supplementary Material S2). These results can be interpreted by considering that the rate-limiting step involves a diffusion-controlled electron transfer between cytochrome c_2 and the bacterial peroxidase, associated with conformational changes [44]. However, the possibility that glycerol is working as an osmolyte cannot be ruled out. Although, the percentage of glycerol used is not expected to destabilize the proteins, it could on the other hand stabilize them in a conformation that is not suitable for electron transfer.

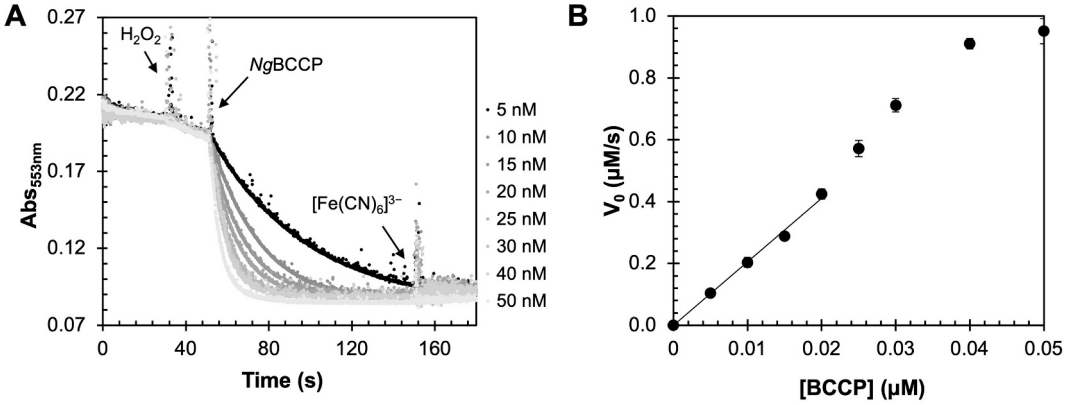

Fig. 2. Effect of enzyme concentration on cytochrome c_2-mediated bacterial peroxidase catalytic activity. Panel **(A)** shows the kinetic traces of the oxidation of cytochrome c_2 in assays initiated with different amounts of enzyme, from black (5 nM) to light grey (50 nM). Panel **(B)** shows the initial velocity determined from the traces in panel (A). The linear regression of V_0 *versus* [BCCP] up to 20 nM has a slope of 20.5 ± 0.4 s^{-1} and a correlation coefficient of 0.999.

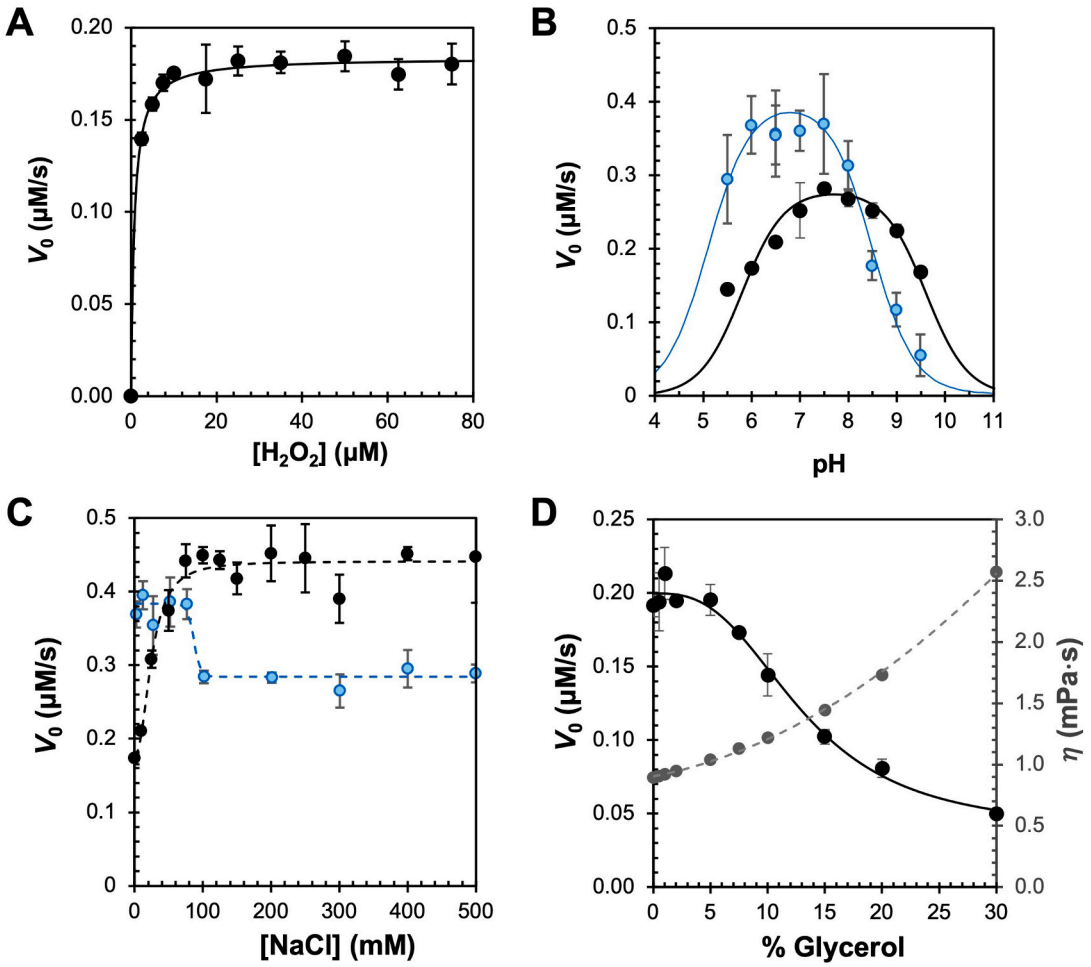

Fig. 3. Steady-state kinetics of *N. gonorrhoeae* bacterial peroxidase using cytochrome c_2 as electron donor. Cytochrome c_2-mediated bacterial peroxidase activity, as a function of (**A**) increasing concentration of hydrogen peroxide at pH 6.5, (**B**) pH between 5.5 and 9.5, **(C)** ionic strength and (**D**) glycerol. The lines correspond to the curves using the Michaelis-Menten equation and Eq. (1) and the parameters stated in the main text. The data and lines in blue are the data and fit obtained for the LAz-mediated bacterial peroxidase activity [14]. (For interpretation of the references to color in this figure legend, the reader is referred to the web version of this article.)

3.2. Molecular docking simulation

Two docking algorithms, the ZDOCK ("hard-docking") [51,77] and the HADDOCK ("soft-docking") were used to obtain a structural model of the bacterial peroxidase/cytochrome c_2 competent electron-transfer complex. The structural model of this complex was also obtained using AlphaFold3. In most of the top 150 models generated by ZDOCK, cytochrome c_2 was positioned near the exposed bacterial peroxidase E heme, while in a few solutions it was located at the dimer interface (Fig. 4A). In 78 of the 150 models, the distance between the E heme iron of bacterial peroxidase and the heme iron of cytochrome c_2 was less than 20 Å, which is generally considered the upper limit for effective electron-transfer [45,46]. The "soft-docking" performed with HADDOCK clustered 118 models into 14 clusters, representing 59 % of the water-refined models generated. Of these 118 models, 40 featured a distance between the heme iron of cytochrome c_2 and the E heme iron of bacterial peroxidase of less than 20 Å (Fig. 4B). In all the AlphaFold3 generated models, cytochrome c_2 is positioned very close to the E heme (Fig. 4C).

The top 5 models obtained with either ZDOCK, HADDOCK or AlphaFold3 algorithms were analyzed with PDBePISA to obtain the geometrical and physiochemical properties of the protein-protein interface and heme iron distances (Table 1 and Fig. S6, S7and S8 in Supplementary Materials S4). The distance between the heme irons of cytochrome c_2 and bacterial peroxidase E heme was less than 20 Å (Table 1) for all the models, but in the AlphaFold models the distance between the heme edges is larger than for the other complexes, being between 8 and 9 Å (Fig. S9 and S10 in Supplementary Materials). The variation of the accessible surface area was determined to be in the range 816–1147 $Å^2$ for ZDOCK models, 644–804 $Å^2$ for HADDOCK models and 412–672 $Å^2$ for AlphaFold3 models (Table 1). Furthermore, in these top models, there is a negative solvation-free energy gain (Δ^iG) upon complex formation (−11.2 to −4.8 kcal.mol^{-1}), a large proportion of apolar residues (40 % – 61 %) and a large number of hydrogen-bonds (average of 8, 4 and 2 for ZDOCK, HADDOCK, and AlphaFold3, respectively), with only a few salt-bridges identified specially in the ZDOCK models (Table 1).

Compared to the characterized electron transfer complex involving *N. gonorrhoeae* bacterial peroxidase and LAz [14], the electron-transfer complexes generated here shows a lower percentage of apolar residues at the interface (~60 % for LAz), but similar number of salt bridges (0–2 for LAz).

All the complexes generated by ZDOCK, HADDOCK and AlphaFold3 show similar interface regions that involve α-helices and loop sections around the *c*-type heme of both proteins and have a hydrophobic character (Fig. 5). This further supports the proposal that the surface in electron-transfer complexes around the redox centers is hydrophobic to promote a more efficient electron-transfer process [47,48].

The disordered C-terminal region of cytochrome c_2 was found to be

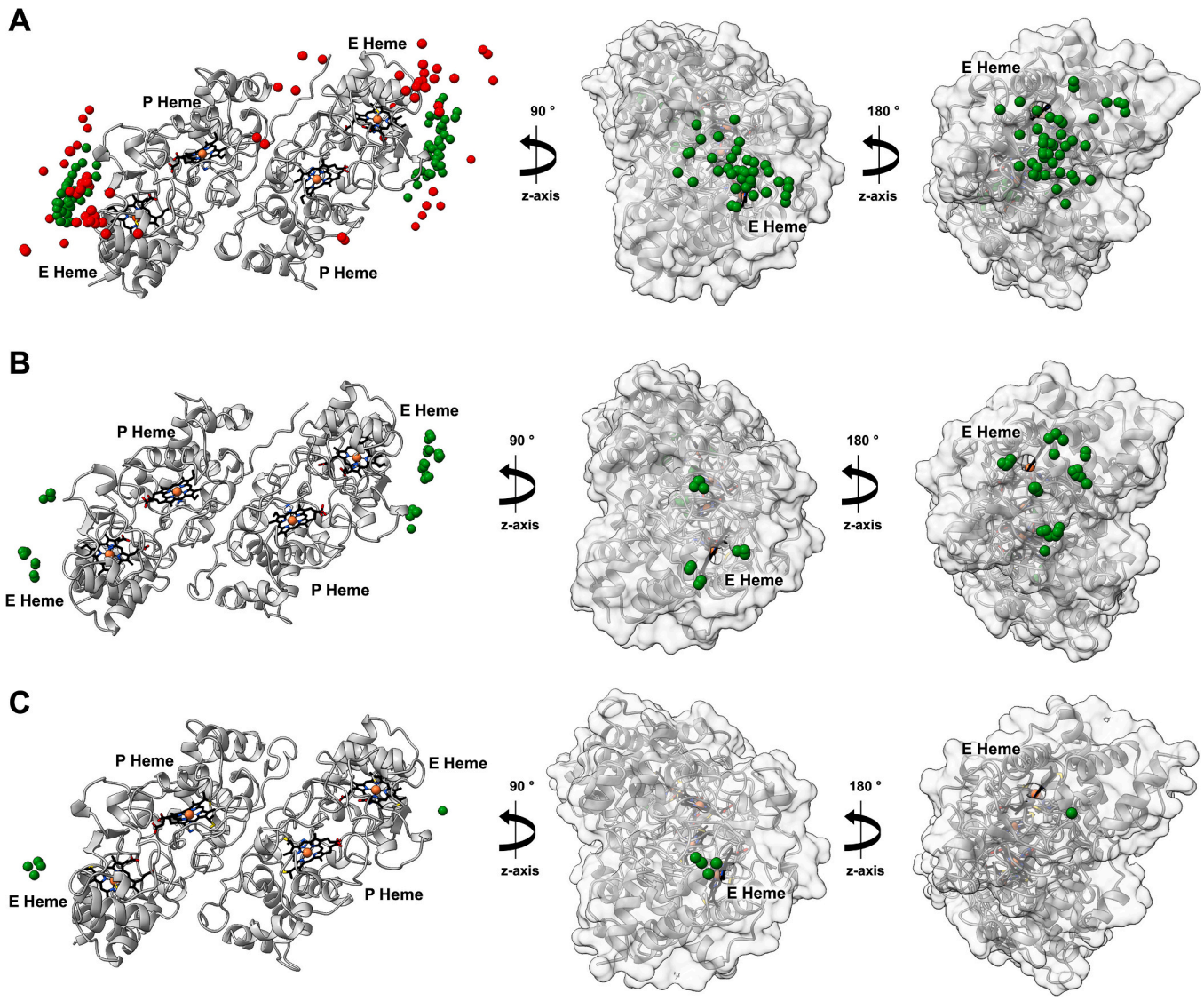

Fig. 4. Molecular docking of cytochrome c_2 to bacterial peroxidase dimer using **(A)** ZDOCK, **(B)** HADDOCK and **(C)** AlphaFold3 algorithms. The top 150 solutions, 14 solutions clusters, and 5 models represented by cytochrome c_2 heme iron atom position as green/red spheres, are shown in Panel A, B, and C, respectively. The heme iron atoms within 20 Å from the E heme iron are represented by green spheres and the others by red spheres. The E and P heme iron atoms of the bacterial peroxidase are displayed as spheres in salmon, the hemes are shown as black sticks and bacterial peroxidase backbone is represented as white ribbons (left) or surface (right). (For interpretation of the references to color in this figure legend, the reader is referred to the web version of this article.)

involved in the binding interface of the ZDOCK and HADDOCK models, while in the model complexes generated by AlphaFold3, the algorithm modeled this region away from the interface (Fig. S8 in Supplementary Materials S4).

4. Discussion

4.1. Cytochrome c_2 is an efficient electron donor to the bacterial peroxidase from Neisseria gonorrhoeae

N. gonorrhoeae cytochrome c_2 is a small periplasmic *c*-type cytochrome proposed to transfer electrons to the copper containing nitrite reductase [27]. The copper containing nitrite reductase is an outer membrane copper nitrite reductase that enables growth under low oxygen conditions by utilizing nitrite as terminal electron acceptor [18,49]. However, under these conditions, respiration is inefficient, leading to electron leakage and the production of superoxide anion, which is subsequently converted into hydrogen peroxide [43,50]. *N. gonorrhoeae* bacterial peroxidase is an outer-membrane-bound enzyme that is also produced under low oxygen conditions, as the *ccp* gene is under the control of FNR [10], and catalyzes the reduction of hydrogen peroxide to water. This reaction requires electrons delivered by small periplasmic shuttle proteins, and LAz has been identified as capable of fulfilling this role [14,15].

The ability of periplasmic oxidoreductases to receive electrons from multiple donors has been reported in other organisms [20,25,29,30]. Since both the bacterial peroxidase and cytochrome c_2 are produced under oxygen limiting conditions [10,27], we investigated whether cytochrome c_2 could also act as an electron donor to that enzyme *in vitro*.

Our results demonstrate that cytochrome c_2 can efficiently transfer electrons to the bacterial peroxidase, with a k_{obs} of 18 ± 1 s^{-1} and a K_M, for H_2O_2, of 0.74 ± 0.08 μM at pH 6.5. These kinetic parameters are of the same order of magnitude as those obtained for the *N. gonorrhoeae* LAz/BCCP pair (K_M of 0.4 ± 0.2 μM for H_2O_2 and a k_{obs} of 39 s^{-1}, at pH 6.0) [14], supporting the hypothesis that both proteins could be physiological electron donors of the *N. gonorrhoeae* bacterial peroxidase.

A comparative analysis of the effect of pH and ionic strength on the mediated bacterial peroxidase catalytic activity provides further insights

Table 1
Geometrical and physicochemical characteristics of the top five models obtained with ZDOCK, HADDOCK and AlphaFold3 algorithms. The models were analyzed with PDBePISA.

Model ZDOCK	Score	Fe-Fe distance (Å)	ΔASA[a] (Å²)	Δ[i]G[b] (kcal/mol)	Apolar residues (%)	H-bonds / Salt Bridges
1	1233	15.3	1147	- 11.2	40	12 / 2
2	1127	15.9	1112	- 8.6	43	12 / 5
3	997	15.9	957	- 7.5	42	5 / 0
4	991	15.4	942	- 8.5	47	5 / 2
5	986	15.8	816	- 5.8	47	4 / 0
Model HADDOCK	**Score**	**Fe-Fe distance (Å)**	**ΔASA[a] (Å²)**	**Δ[i]G[b] (kcal/mol)**	**Apolar residues (%)**	**H-bonds / Salt Bridges**
1	- 91	16.7	729	- 10.7	48	4 / 1
2	- 83	17.3	804	- 8.6	47	5 / 0
3	- 80	16.4	719	- 10.7	45	4 / 0
4	-78	17.6	753	- 8.0	45	3 / 0
5	- 76	16.9	644	- 9.7	61	4 / 1
Model AlphaFold	**Score**	**Fe-Fe distance (Å)**	**ΔASA[a] (Å²)**	**Δ[i]G[b] (kcal/mol)**	**Apolar residues (%)**	**H-bonds / Salt Bridges**
1	–	17.2	564	- 6.9	48	1 / 0
2	–	18.2	473	- 6.5	55	3 / 0
3	–	17.7	563	- 6.7	51	3 / 0
4	–	17.8	672	- 6.7	43	3 / 0
5	–	18.8	415	- 4.8	55	1 / 0

[a] ASA – Accessible surface area.
[b] Δ[i]G – Solvation energy gain.

on why two electron shuttle proteins may be required. Although the assays were performed with different electron donor concentrations, the activity profile show that the optimum pH is higher when cytochrome c_2 is the donor, potentially sustaining enzyme activity under slightly basic environmental conditions, such as those encountered at the intracellular pH of host cells. More striking is the effect of ionic strength, as there is a 2.3-fold increase in activity at NaCl concentrations above 100 mM NaCl. At this NaCl concentration, activity is 1.5-fold higher with cytochrome c_2 than with LAz as electron donor (Fig. 2C). This difference is particularly relevant given that the ionic strength of the periplasm is expected to be within the physiological range (150 mM), and influenced by the external environment [51].

The two p*Ka* values found in the pH-profile, pKa_1 of 5.8 ± 0.2 and pKa_2 of 9.6 ± 0.1, are slightly higher than those obtained for the *N. gonorrhoeae* LAz/BCCP pair (pKa_1 of 5.1 ± 0.1 and a pKa_2 of 8.5 ± 0.1) [14] or for *N. gonorrhoeae* bacterial peroxidase when assayed with an artificial electron donor (pKa_1 of 5.9 ± 0.1 and a pKa_2 of 8.4 ± 0.1) [12]. A bell-shaped activity profile has been reported for bacterial peroxidases from different microorganisms, such as *Nitrosomonas europaea* (electrochemistry: 6.5/8.4) [52], *P. aeruginosa* (cytochrome c_{551}: 4.4/7.0) [25], *R. capsulatus* (cytochrome c_{552}: 6.1/7.9) [53], and *Geobacter sulfurreducens* (CcpA/$ABTS^{2-}$: 5/8) [54].

In mediated catalysis, the rate-limiting step is the formation of the electron-transfer complex, and thus the pH dependence may reflect a composite effect of binding and electron transfer. Therefore, direct assignment of the observed p*Ka* values to specific residues is challenging. The observed p*Ka* values are generally attributed to ionizable groups that are critical for catalysis, and thus in this case it is tempting to assign the lower p*Ka* value to the conserved residue in the catalytic pocket (Glu118 for *N. gonorrhoeae*), proposed to act as the acid-base catalytic group that leads to the heterolytic cleavage of the peroxide O—O bond and donates the first proton for the release of the first water molecule [17,55,56]. However, considering the electron transfer complex formed between *N. gonorrhoeae* bacterial peroxidase and cytochrome c_2, the lower apparent p*Ka* value around 6 may correspond to protonation of the heme propionate groups of E heme bacterial peroxidase and cytochrome c_2. Protonation of these groups can modulate the reduction of the heme and alter the electron transfer rate. The variability in the reported lower p*Ka* values for electron transfer complexes involving cytochrome *c* and bacterial peroxidases from different organisms, likely reflects differences in experimental conditions (buffer composition, ionic strength).

The higher p*Ka* value of 9.6 may arise from a residue that must remain protonated for maximal activity and likely corresponds to a surface-exposed residue in the *N. gonorrhoeae* bacterial peroxidase that contributes to complex formation. Notably, lysine residues are observed at the protein–protein interface in docking models of the bacterial

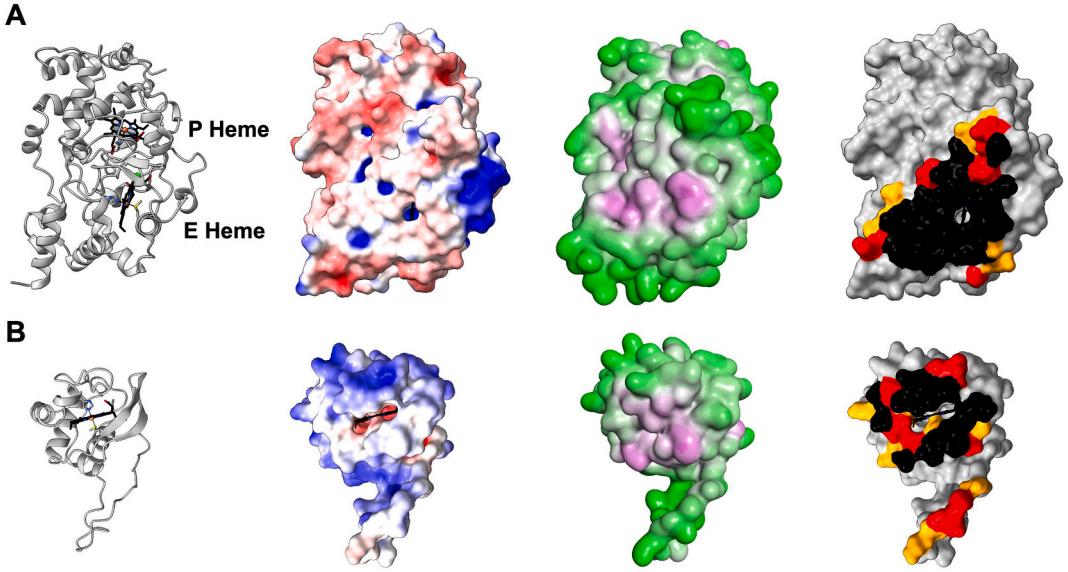

Fig. 5. The interface of **(A)** bacterial peroxidase and **(B)** cytochrome c_2, colored according to the frequency that each residue occurs in the interface of the top ZDOCK, HADDOCK and AlphFold3 models (> 75 % models in black; 50–75 % models in red; 25–50 % models in orange). The second and third images in each panel show the surface of the proteins colored according to its electrostatic potential (form – 5 (red) to +5 kT/e (blue)) and hydrophobicity (from purple (hydrophobic) to green (hydrophilic)). The monomer of the bacterial peroxidase is shown for simplicity. (For interpretation of the references to color in this figure legend, the reader is referred to the web version of this article.)

peroxidase with either LAz or cytochrome c_2, with Lys216 and Lys287 appearing in approximately 75 % of the top-ranked complexes and Lys243 in about 50 %. These positively charged residues can influence association, orientation, and/or stabilization of the electron-transfer complex. Nevertheless, assigning the observed p*Ka* value to a specific residue remains tentative. Definitive validation will require additional experiments using site-directed variants of these lysines to determine their contribution to complex formation and catalytic efficiency.

4.2. The electron-transfer complex between cytochrome c_2 and bacterial peroxidase

The dependence of the activity on ionic strength and viscosity suggests that the electron-transfer complex has a hydrophobic character and that its formation is not simply diffusion-controlled. A α value of 1.5 for the viscosity dependence of catalytic activity (Fig. S4, in Supplementary Materials S2) indicates that solvent viscosity influences conformational motions required to form a productive electron-transfer geometry. Such motions likely include lateral or rotational diffusion of the proteins along each other's surfaces, a process that has been proposed for several redox complexes [19,48,57]. Increasing viscosity slows these conformational motions and may also shift the ensemble of encounter orientations. Consequently, glycerol could stabilize non-productive or misaligned orientations of the complex, thereby decreasing the probability of forming the catalytically competent electron-transfer arrangement.

The binding interface of the electron-transfer complex is mainly hydrophobic and includes a few positive and negatively charged residues (Fig. 5C, and Table 1), which may need to be shielded for a more efficient electron transfer, explaining the increase of activity up to 100 mM NaCl.

The existence of positively charged patches on the cytochrome c_2 surface is likely crucial to guide the docking and formation of the initial "encounter complex", as efficient electron-transfer reactions require precise orientation of donor and acceptor redox centers [19,48,57]. However, these charged patches are less pronounced than those reported for *P. pantotrophus* pseudoazurin and cytochrome c_{550}, both redox partners of the bacterial peroxidase from this organism [20]. This difference may contribute to lower binding affinities in *Neisseria* complexes, which could result in a higher K_D. This could also explain why these complexes are difficult to characterize using NMR titration experiments [14], as multiple orientations and microstates might occur without specific binding [57], even when docking programs identify a preferred binding position.

The transient nature of these interactions is further supported by the relatively small contact area [47,48,58] observed in the docking models of cytochrome c_2/bacterial peroxidase. Furthermore, the flexible and disordered C-terminal region of cytochrome c_2 may represent an evolutionary strategy that facilitates interactions with multiple redox partners under physiological context, such as the bacterial peroxidase and the nitrite reductase under low oxygen conditions.

4.3. The electron-transfer pathway

The docking models were analyzed using the eMAP webserver to identify potential electron-transfer pathways between the two proteins. No conserved pathway was identified among the top-ranked docking models, reflecting the different possible docking geometries and the transient and dynamic nature of the complex. Moreover, the analysis of these models supports the proposal that electron transfer can occur *via* direct through-space tunnelling between the *c*-type heme centers, without the involvement of residues, as the distance between the E heme methyl-3 (bacterial peroxidase) and the heme methyl-4 (cytochrome c_2) averages at 5–4 Å (Fig. S9 in Supplementary Materials S4). Such tunnelling pathways are known to support rapid electron transfer due to strong electronic coupling and reduced energetic barriers, consistent with established principles of biological electron transfer [46,59,60].

5. Conclusions

Cytochrome c_2 from *N. gonorrhoeae* efficiently donates electrons to the organism's own bacterial peroxidase. This suggests a possible link between the truncated denitrification pathway and the reduction of hydrogen peroxide, which are both likely to occur simultaneously during infection. To support this hypothesis, it has been shown that hydrogen peroxide inhibits copper nitrite reductases [61], and their co-occurrence be an extra defense mechanism given the importance of maintaining the copper nitrite reductase functional for gonococcal infection [62].

Steady-state kinetics were employed to study the cytochrome c_2-mediated catalysis of *N. gonorrhoeae* bacterial peroxidase, and the estimated kinetic parameters were found to be comparable to those determined for LAz-mediated catalysis. This finding lends weight to the idea that small periplasmic redox proteins can act as substitutes for one another and perform interchangeable functions. In this case, the dependence on pH and ionic strength further suggests the advantage of an alternative electron donor, enabling the gonococcus to adapt to variable environmental conditions.

The electron-transfer complex between cytochrome c_2 and the bacterial peroxidase is stabilized by hydrophobic interactions, facilitating rapid electron turnover at physiological pH, even in the event of minor environmental changes. Kinetic studies also support the transient nature of this complex, with cytochrome c_2 sampling multiple conformations across the bacterial peroxidase surface.

A similar dynamic complex was observed for the LAz complex, which binds to the same surface on the peroxidase. However, given that *N. gonorrhoeae* bacterial peroxidase is anchored to the outer membrane on the periplasmic side, the orientation of the electron-transfer complex *in vivo* is constrained. These constraints are likely to be more significant for the *N. gonorrhoeae* LAz/BCCP complex, as both proteins are membrane anchored. In contrast, the soluble, periplasmic nature of cytochrome c_2 allows greater conformational flexibility, and more degrees of freedom for complex formation with the bacterial peroxidase. Competition studies between these two proteins as electron donors to the bacterial peroxidase are therefore essential to determine the conditions under which one complex predominates.

Overall, the findings presented here contribute to a more detailed understanding of electron-transfer-driven protein-protein interactions in the periplasm of *N. gonorrhoeae*, particularly in response to exogenous H_2O_2.

CRediT authorship contribution statement

Pedro M.S. Bragança: Writing – original draft, Visualization, Investigation, Formal analysis. **Daniela S. Barreiro:** Formal analysis, Investigation, Software, Visualization, Writing – review & editing. **Marta S.P. Carepo:** Writing – review & editing, Validation, Supervision, Methodology. **Sofia R. Pauleta:** Writing – review & editing, Writing – original draft, Visualization, Validation, Supervision, Project administration, Funding acquisition, Formal analysis, Data curation, Conceptualization.

Declaration of competing interest

The authors declare the following financial interests/personal relationships which may be considered as potential competing interests:

Acknowledgements

The authors acknowledge Fundação para a Ciência e a Tecnologia (FCT) for funding the projects PTDC/BIA-PRO/109796/2009 and PTDC/BIA-BQM/29442/2017 to SRP, UCIBIO (UIDP/04378/2020 and

UIDB/04378/2020), and Associate Laboratory for Health and Bio-economy-i4HB (LA/P/0140/2020), Associate Laboratory for Green Chemistry - LAQV (UIDP/50006/2020, UIDB/50006/2020 and LA/P/0008/2020), and the PhD grant attributed to PMSB (PD/BD/150979/2021, under the PTNMRPhD program PD00065/2013) and DSB (UI/BD/151168/2021).

Appendix A. Supplementary data

Supplementary data to this article can be found online at https://doi.org/10.1016/j.jinorgbio.2025.113164.

References

[1] M. Unemo, H.S. Seifert, E.W. Hook 3rd, S. Hawkes, F. Ndowa, J.R. Dillon, Nat. Rev. Dis. Primers 5 (2019) 79.
[2] M. Unemo, J. Ahlstrand, L. Sanchez-Buso, M. Day, D. Aanensen, D. Golparian, S. Jacobsson, M.J. Cole, M.J. Borrego, G. European Collaborative, J. Antimicrob. Chemother. 76 (2021) 1221–1228.
[3] E. Walker, S. van Niekerk, K. Hanning, W. Kelton, J. Hicks, Front. Microbiol. 14 (2023) 1119834.
[4] A.E. Sikora, R.H. Mills, J.V. Weber, A. Hamza, B.W. Passow, A. Romaine, Z. A. Williamson, R.W. Reed, R.A. Zielke, K.V. Korotkov, Antimicrob. Agents Chemother. 61 (2017).
[5] W.J. Kim, D. Higashi, M. Goytia, M.A. Rendon, M. Pilligua-Lucas, M. Bronnimann, J.A. McLean, J. Duncan, D. Trees, A.E. Jerse, M. So, Cell Host Microbe 26 (2019) 228–239 e228.
[6] K.L. Seib, H.J. Wu, S.P. Kidd, M.A. Apicella, M.P. Jennings, A.G. McEwan, Microbiol. Mol. Biol. Rev. 70 (2006) 344–361.
[7] K.L. Seib, H.J. Wu, Y.N. Srikhanta, J.L. Edwards, M.L. Falsetta, A.J. Hamilton, T. L. Maguire, S.M. Grimmond, M.A. Apicella, A.G. McEwan, M.P. Jennings, Mol. Microbiol. 63 (2007) 54–68.
[8] S. Lissenden, S. Mohan, T. Overton, T. Regan, H. Crooke, J.A. Cardinale, T. C. Householder, P. Adams, C.D. O'Conner, V.L. Clark, H. Smith, J.A. Cole, Mol. Microbiol. 37 (2000) 839–855.
[9] J.A. Cole, Microbiology 158 (2012) 1402–1413.
[10] R.N. Whitehead, T.W. Overton, L.A. Snyder, S.J. McGowan, H. Smith, J.A. Cole, N. J. Saunders, BMC Genomics 8 (2007) 35.
[11] S.R. Johnson, B.M. Steiner, D.D. Cruce, G.H. Perkins, R.J. Arko, Infect. Immun. 61 (1993) 1232–1238.
[12] C.S. Nobrega, M. Raposo, G. Van Driessche, B. Devreese, S.R. Pauleta, J. Inorg. Biochem. 171 (2017) 108–119.
[13] S. Turner, E. Reid, H. Smith, J. Cole, Biochem. J. 373 (2003) 865–873.
[14] C.S. Nobrega, S.R. Pauleta, FEBS Lett. 592 (2018) 1473–1483.
[15] C.S. Nobrega, I.H. Saraiva, C. Carreira, B. Devreese, M. Matzapetakis, S.R. Pauleta, Biochim. Biophys. Acta 1857 (2016) 169–176.
[16] K.L. Seib, H.J. Tseng, A.G. McEwan, M.A. Apicella, M.P. Jennings, J. Infect. Dis. 190 (2004) 136–147.
[17] C.S. Nobrega, A.L. Carvalho, M.J. Romao, S.R. Pauleta, Int. J. Mol. Sci. 24 (2023).
[18] D.S. Barreiro, R.N.S. Oliveira, S.R. Pauleta, Biomolecules 13 (2023).
[19] G.W. Pettigrew, A. Echalier, S.R. Pauleta, J. Inorg. Biochem. 100 (2006) 551–567.
[20] S.R. Pauleta, A. Cooper, M. Nutley, N. Errington, S. Harding, F. Guerlesquin, C. F. Goodhew, I. Moura, J.J. Moura, G.W. Pettigrew, Biochemistry 43 (2004) 14566–14576.
[21] S.R. Pauleta, F. Guerlesquin, C.F. Goodhew, B. Devreese, J. Van Beeumen, A. S. Pereira, I. Moura, G.W. Pettigrew, Biochemistry 43 (2004) 11214–11225.
[22] W. Hu, L. De Smet, G. Van Driessche, R.G. Bartsch, T.E. Meyer, M.A. Cusanovich, J. Van Beeumen, Eur. J. Biochem. 258 (1998) 29–36.
[23] G.S. Pulcu, K.E. Frato, R. Gupta, H.R. Hsu, G.A. Levine, M.P. Hendrich, S.J. Elliott, Biochemistry 51 (2012) 974–985.
[24] C.G. Timoteo, P. Tavares, C.F. Goodhew, L.C. Duarte, K. Jumel, F.M. Girio, S. Harding, G.W. Pettigrew, I. Moura, J. Biol. Inorg. Chem. 8 (2003) 29–37.
[25] R. Soininen, N. Ellfolk, Acta Chem. Scand. 26 (1972) 861–872.
[26] J.A. Zahn, D.M. Arciero, A.B. Hooper, J.R. Coats, A.A. DiSpirito, Arch. Microbiol. 168 (1997) 362–372.
[27] A.C. Hopper, Y. Li, J.A. Cole, J. Bacteriol. 195 (2013) 2518–2529.
[28] H.J. Wu, K.L. Seib, J.L. Edwards, M.A. Apicella, A.G. McEwan, M.P. Jennings, Infect. Immun. 73 (2005) 8444–8448.
[29] M. Koutny, I. Kucera, R. Tesarik, J. Turanek, R.J. Van Spanning, FEBS Lett. 448 (1999) 157–159.
[30] I.V. Pearson, M.D. Page, R.J. van Spanning, S.J. Ferguson, J. Bacteriol. 185 (2003) 6308–6315.
[31] C.F. Goodhew, K.R. Brown, G.W. Pettigrew, Biochimica et Biophysica Acta (BBA) - Bioenergetics 852 (1986) 288–294.
[32] J.B. Segur, H.E. Oberstar, Ind. Eng. Chem. 43 (1951) 2117–2120.
[33] R.A. Alberty, V. Bloomfield, J. Biol. Chem. 238 (1963) 2804–2810.
[34] N.A. Baker, D. Sept, S. Joseph, M.J. Holst, J.A. McCammon, Proc. Natl. Acad. Sci. USA 98 (2001) 10037–10041.
[35] I. Lotan, T. Head-Gordon, J. Chem. Theory Comput. 2 (2006) 541–555.
[36] T.J. Dolinsky, J.E. Nielsen, J.A. McCammon, N.A. Baker, Nucleic Acids Res. 32 (2004) W665–W667.
[37] B.G. Pierce, K. Wiehe, H. Hwang, B.H. Kim, T. Vreven, Z. Weng, Bioinformatics 30 (2014) 1771–1773.
[38] R.V. Honorato, M.E. Trellet, B. Jimenez-Garcia, J.J. Schaarschmidt, M. Giulini, V. Reys, P.I. Koukos, J. Rodrigues, E. Karaca, G.C.P. van Zundert, J. Roel-Touris, C. W. van Noort, Z. Jandova, A.S.J. Melquiond, A. Bonvin, Nat. Protoc. 19 (2024) 3219–3241.
[39] J. Abramson, J. Adler, J. Dunger, R. Evans, T. Green, A. Pritzel, O. Ronneberger, L. Willmore, A.J. Ballard, J. Bambrick, S.W. Bodenstein, D.A. Evans, C.C. Hung, M. O'Neill, D. Reiman, K. Tunyasuvunakool, Z. Wu, A. Zemgulyte, E. Arvaniti, C. Beattie, O. Bertolli, A. Bridgland, A. Cherepanov, M. Congreve, A.I. Cowen-Rivers, A. Cowie, M. Figurnov, F.B. Fuchs, H. Gladman, R. Jain, Y.A. Khan, C.M. R. Low, K. Perlin, A. Potapenko, P. Savy, S. Singh, A. Stecula, A. Thillaisundaram, C. Tong, S. Yakneen, E.D. Zhong, M. Zielinski, A. Zidek, V. Bapst, P. Kohli, M. Jaderberg, D. Hassabis, J.M. Jumper, Nature 630 (2024) 493–500.
[40] E. Krissinel, K. Henrick, J. Mol. Biol. 372 (2007) 774–797.
[41] S. Jones, J.M. Thornton, Proc. Natl. Acad. Sci. USA 93 (1996) 13–20.
[42] R.N. Tazhigulov, J.R. Gayvert, M. Wei, K.B. Bravaya, J. Phys. Chem. B 123 (2019) 6946–6951.
[43] C.S. Nobrega, S.R. Pauleta, Adv. Microb. Physiol. 74 (2019) 415–464.
[44] C. Feng, R.V. Kedia, J.T. Hazzard, J.K. Hurley, G. Tollin, J.H. Enemark, Biochemistry 41 (2002) 5816–5821.
[45] J.R. Winkler, Curr. Opin. Chem. Biol. 4 (2000) 192–198.
[46] R.A. Marcus, N. Sutin, Biochimica et Biophysica Acta (BBA) - Reviews on Bioenergetics 811 (1985) 265–322.
[47] P.B. Crowley, M.A. Carrondo, Proteins 55 (2004) 603–612.
[48] A.N. Volkov, Acc. Chem. Res. 48 (2015) 3036–3043.
[49] B.I. Baarda, R.A. Zielke, A.E. Jerse, A.E. Sikora, Front. Microbiol. 9 (2018) 2915.
[50] D.S. Barreiro, R.N.S. Oliveira, S.R. Pauleta, Coord. Chem. Rev. 485 (2023).
[51] J.B. Stock, B. Rauch, S. Roseman, J. Biol. Chem. 252 (1977) 7850–7861.
[52] A.L. Bradley, S.E. Chobot, D.M. Arciero, A.B. Hooper, S.J. Elliott, J. Biol. Chem. 279 (2004) 13297–13300.
[53] M. Koh, T.E. Meyer, L. De Smet, J.J. Van Beeumen, M.A. Cusanovich, Arch. Biochem. Biophys. 410 (2003) 230–237.
[54] M. Hoffmann, J. Seidel, O. Einsle, J. Mol. Biol. 393 (2009) 951–965.
[55] A. Echalier, C.F. Goodhew, G.W. Pettigrew, V. Fulop, Structure 14 (2006) 107–117.
[56] A. Echalier, T. Brittain, J. Wright, S. Boycheva, G.B. Mortuza, V. Fulop, N. J. Watmough, Biochemistry 47 (2008) 1947–1956.
[57] Q. Bashir, S. Scanu, M. Ubbink, FEBS J. 278 (2011) 1391–1400.
[58] L. Lo Conte, C. Chothia, J. Janin, J. Mol. Biol. 285 (1999) 2177–2198.
[59] H.B. Gray, J.R. Winkler, Proc. Natl. Acad. Sci. USA 102 (2005) 3534–3539.
[60] C.C. Page, C.C. Moser, X. Chen, P.L. Dutton, Nature 402 (1999) 47–52.
[61] T.J. Lawton, K.E. Bowen, L.A. Sayavedra-Soto, D.J. Arp, A.C. Rosenzweig, J. Biol. Chem. 288 (2013) 25575–25583.
[62] P. Muenzner, C.R. Hauck, Cell Host Microbe 27 (2020) 793–808 e795.